Laser–Electron X-Ray Source for Medical Applications

E. G. Bessonov, A. V. Vinogradov, and A. G. Tourianskii

Lebedev Physical Institute, Russian Academy of Sciences, Leninskii pr. 53, Moscow, 119991 Russia

Received November 30, 2001

Abstract—A specialized source of quasi-monochromatic X-ray radiation for medical application is proposed. It includes two electron storage rings ($E \approx 50$ MeV) placed in the vertical plane and two laser resonators located in the horizontal and vertical planes. Hard X rays are generated in a process of back Compton scattering of laser photons ~1eV by electrons in the linear paths of storage rings. The scheme of the X-ray beam sweeping over the predetermined region of interest for two-dimensional imaging is described. The possibility of multifold increasing of the noise-to-signal ratio and decreasing radiation doses for patients and personnel is shown.

1. INTRODUCTION

Almost exceptionally, vacuum X-ray tubes are used in modern medical practice as sources of X rays. This is determined by the simplicity of their design and also by the capability of altering in the wide range such basic parameters as the power, effective spectrum energy, the pulse duration, and the size of the focus depending on a diagnostic problem. In addition, tubes provide an acceptable homogeneity of the radiation flux density in a wide space angle, thus making it possible to obtain two-dimensional (2D) images of any part of patient's body.

At present, a change to digital techniques for detecting X-ray images using detecting linear arrays and matrices [1, 2] is being developed. In this process, attention is mainly paid to obtaining a maximum amount of information at a minimum dosimetric load. In the context of solving this task, significant problems are concerned with the fact that the X-ray tube radiation spectrum $P(\varepsilon)$ (ε is the photon energy) is polychromatic and contains both bremsstrahlung and characteristic lines. For example, at a 120-kV voltage across a tube with a 2-mm-thick Al filter, the photon energy is distributed within the range of 20–120 keV [3]. In this case, $P(\varepsilon)$ continuously changes, as the radiation passes through the investigated object. Editing of the reconstruction algorithm [4] is required in computer tomography for taking into account the beam polychromaticity and evolution of its spectrum.

It is known that a change to monochromatic or quasi-monochromatic radiation could significantly improve the quality of obtained images and increase the accuracy of a 3D object reconstruction [5]. It is possible to simultaneously achieve a decrease in the surface (skin) radiation dose and in the total radiation dose of the patient and medical personnel without detriment to the informativeness of diagnostic procedures [6].

Let us estimate the energy flux of X rays through a zone S with a size of 30×30 cm^2 typical of medical investigations. In widespread X-ray industrial and medical facilities, the power of X-ray tubes in a steady-state regime (>1 min) is within 4–5 kW. The efficiency of electron-beam power conversion into a cumulative flux of bremsstrahlung and fluorescent radiation at a voltage $U_t \sim 100$ kV across the tube is usually 0.1–0.5% [7, 8]. Considering the primary flux excited in the focus isotropic and choosing the average value of the conversion efficiency, we obtain a flux through the zone S equal to $\Phi_S \approx 0.03$ W at a distance of 1 m from the tube and an electric power $P_t = 1$ kW. According to [3], at $U_t \sim 100$ kV, the average quanta energy in the spectrum of medical tubes taking into consideration the action of filters, which absorb a soft portion of the spectrum, is about $E_q \approx 40$ keV. The quanta flux through the S zone at the stated P_t and E_q is $\Phi_S \approx 5 \times 10^{12}$ s^{-1}. For tubes with the rotating anode used in computer tomography, P_t may reach 20 kW in a short-time duty (<5 s), and the corresponding flux value is $\Phi_S \approx 10^{14}$ s^{-1}. In practice, the values of Φ_S can be significantly lower as a result of an absorption in additional filters installed on the output window of the radiator.

As follows from our estimates, the monochromatization of the tube's radiation by selecting a band $\Delta E \sim 1$ keV by means of crystal monochromators will lead to an additional loss in the useful radiation power by at least three orders of magnitude. This is associated with the following factors: (a) a relatively low yield of K-series fluorescence for the tungsten anode [9], which is commonly used in medical tubes; (b) losses during the selection of the spectral band by crystal monochromators; and (c) a significant decrease in the space angle, into which the working radiation flux is directed during the monochromatization. In this case, a necessity of linear scanning appears in order to obtain images of the aforementioned typical investigation zone with an area $\sim S$.

Thus, taking into account the above considerations, the formation of a monochromatic beam with the power necessary for medical purposes requires an electric

power of a radiator with an electron-excited anode of ~1 MW; however, it seems to be impossible to date.

Note that experimental works for obtaining medical images in monochromatic radiation are currently underway on synchrotrons [10, 11]. However, for the reasons of technical and economical characters (complexity, high price, large dimensions, necessity of numerous maintenance personnel), such devices cannot be used in everyday medical practice. This, particularly, is determined by the fact that an electron energy of >1 GeV is required for obtaining a monochromatic spectrum in a range of 30–60 keV. This can be practically ensured at a diameter of the storage ring of 20–25 m, and a sophisticated and bulky electron acceleration system for subsequent injection into the storage ring is necessary. Moreover, turning of the probe beam into the vertical plane for obtaining patient's base frontal projections (patient is placed horizontally on the operative table) still remains a difficult problem for such systems.

The results of this work show that, when using counter laser and electron beams and sweep X-ray systems, the problem of creating a quasi-monochromatic source which meets the requirements of practical medicine is technically solvable. In particular, as it will be shown below, the electron energy and the size of the storage ring can be reduced by more than an order of magnitude.

2. INVERSE COMPTON EFFECT

The classical Compton effect is a reduction of the photon frequency upon scattering by a free electron at rest. The inverse Compton effect (ICE) is an increase in the photon frequency as a result of scattering by a moving electron. It is precisely the ICE on which the principle of radiation generation by a laser–electron source is based. For counterpropagating beams, the frequency transformation formula has the form

$$\omega = \frac{(1+\beta)\omega_L}{1 - \mathbf{n}\boldsymbol{\beta}}, \tag{1}$$

where $\beta = |\boldsymbol{\beta}|$; $\boldsymbol{\beta} = \mathbf{v}/c$; $\mathbf{v}$ is the particle velocity vector, $\mathbf{n}$ is the unit vector in the direction of observation, c is the light velocity, and ω_L is the frequency of the incident (laser, in our case) radiation.

Expression (1) is valid on the condition that $p_{\perp m} \ll 1$, where $p_{\perp m} = \sqrt{p_{\perp mx}^2 + p_{\perp my}^2}$ is the parameter of electron deflection in the field of an elliptically polarized electric wave, $p_{\perp mx, y}$ are maximum components of the vector of the relative transverse electron momentum, $\mathbf{p}_{\perp} = \boldsymbol{\beta}_{\perp}\gamma$, and $\gamma = 1/\sqrt{1-\beta^2}$ is the relativistic factor of the particle. The components $p_{\perp mx, y} = eE_{Lmx, y}\lambda_L/2\pi mc^2$, where $E_{Lmx, y}$ are the amplitudes of the x and y components of the wave electric field, and $\lambda_L = 2\pi c/\omega_L$ is the laser wavelength [12]. For the fundamental wave mode

Table 1

Electron energy in the storage ring	$\varepsilon = 50$ MeV
Current on the storage-ring orbit	$I = 100$ mA
Average radius of the storage ring	$R = 1$ m
Instantaneous radius of the storage ring	$\bar{R} = 0.5$ m
Frequencies of betatron oscillations	$\nu_{x, y} = 10$
Frequency of the RF resonator ($\lambda = 10.5$ cm)	2856 MHz
Multiplicity	$q = 60$
Voltage at the RF resonator	0.5 MV
$\beta = v/c$	1 cm
Electron energy loss per revolution	6.564 keV
Damping times of amplitudes of radial betatron and phase oscillations	$\tau_{x, z} = 2.04 \times 10^{-3}$ s $\tau_{\varphi} = 1.02 \times 10^{-3}$ s
Equilibrium energy spread	$(\sigma_\varepsilon/\varepsilon) = 1.3 \times 10^{-2}$
Equilibrium normalized transverse emittance	$\varepsilon_x = 17$ nm
Electron beam dimensions:	
transverse	$\sigma_x = \sigma_z = 18.43$ μm
longitudinal	$\sigma_\varphi = 4.22$ mm

$p_{\perp m}^2 = 2I_L\lambda_L^2/\pi P_A$, where $I_L = c(E_{Lmx}^2 + E_{Lmy}^2)/8\pi$ is the intensity of laser radiation, $P_A = m^2c^5/e^2 \cong 8.76$ GW. The amplitudes of the electric and magnetic fields of a circularly polarized plane wave are related to its intensity by the expressions

$$E_{Lmx, y}[\text{V/cm}] \cong 19.416\sqrt{I_L[\text{W/cm}^2]},$$

$$B_{Lmx, y}[\text{G}] \cong 0.0647\sqrt{I_L[\text{W/cm}^2]}.$$

The amplitudes of the intensities for a linearly polarized wave are higher by a factor of $\sqrt{2}$ at the same intensity value.

The sources for which $p_{\perp m} \ll 1$ based on the ICE will be considered below. In the case of photon scattering by a relativistic electron ($\gamma \gg 1$), expression (1) for the frequency of the scattered photon is simplified:

$$\omega = \frac{4\omega_L\gamma^2}{1 + \vartheta^2}, \tag{2}$$

where $\vartheta = \theta\gamma$, θ is an angle of scattering (the angle between the laser-beam axis and the direction of observation).

Note that the beam of the scattered photons is concentrated within a narrow cone $\vartheta \cong 1$ or $\theta \cong 1/\gamma$ along the electron velocity vector. The photons of maximum frequency $\omega_{max} = 4\omega_L\gamma^2$ are emitted in the direction $\vartheta = 0$. It is also clear from formula (2) that, during the interaction of a visible or IR laser beam ($\hbar\omega_L \approx 2$–0.1 eV)

Table 2

Pulse duration	$\tau_L = 1.4 \times 10^{-11}$ s
Pulse energy	$E_L = 2 \times 10^{-3}$ J
Interval between pulses	$T_L = 2 \times 10^{-8}$ s
Train duration (2×10^3 pulses)	$T_1 = 4 \times 10^{-5}$ s
Interval between trains	$T_2 = 8 \times 10^{-2}$ s
Average laser power	$P_L = 50$ W

with relativistic electrons ($\gamma \geq 50$), the ICE leads to a generation X rays.

The averaged flux of X-ray photons at the collision of the counterpropagating electron and laser beams can be estimated by the formula

$$\Phi = \frac{N_L N_e f_e}{S_0}\sigma_T = \frac{N_e \sigma_T}{S_0}\Phi_L, \qquad (3)$$

where N_e is the number of electrons on the orbit of the storage ring, N_L is the number of photons in the laser pulse, f_e is the electron rotation frequency, $\Phi_L = N_L f_L = I_L S_0 / \hbar\omega_L$ is the laser radiation flux, f is laser pulse repetition rate, S_0 is the effective area of the beams' interaction zone, and $\sigma_T = 8\pi r_e^2 / 3 = 6.65 \times 10^{-25}$ cm^2 is the Thomson scattering cross section.

In case of Gaussian beams, $S_0 = S_{0e} + S_{0L}$, where $S_{0e, L} = 2\pi\sigma_{e, L}^2$ are the dispersions of the electron and laser beams in the interaction zone, respectively.
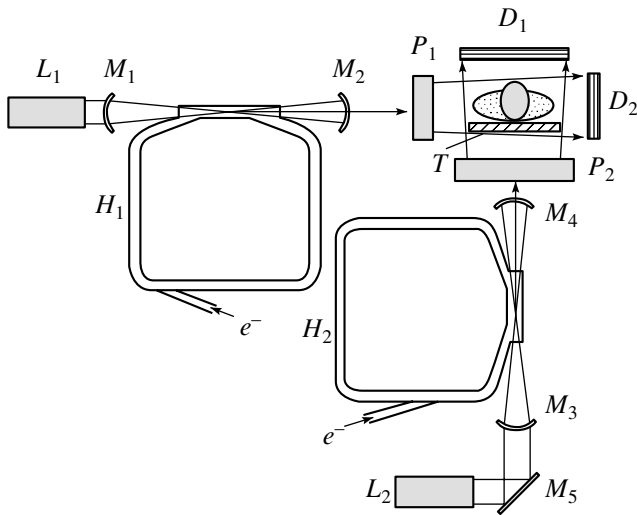
Fig. 1. Schematic of the system for obtaining projections using laser–electron sources: (L_1, L_2) lasers; (H_1, H_2) storage rings for electrons; (M_1, M_2 and M_3, M_4, respectively) focusing mirrors of the horizontal and vertical resonators; (M_5) flat mirror; (P_1, P_2) initial beam sweep systems; (D_1, D_2) detecting units; and (T) patient's table.

In formula (3), we assume that a single electron bunch is located on the orbit, and its rotation frequency coincides with the repetition rate of laser pulses $f_e = f_L$. The interaction of photons and electrons happens in the caustic zone of the laser beam. For this interaction to be effective, the fulfillment of the condition $l > c\tau_L + l_e$ is required, where τ_L is the laser pulse duration, l_e is the bunch length, and $l = S_{0, L}/\lambda$ is the caustic length (Rayleigh length).

The inverse Compton effect during the interaction of electron and electromagnetic beams as a source of short-wavelength radiation was for the first time considered by K. Landeker in 1952 [13]. The first experiments on the ICE observation were carried out on the FIAN (Lebedev Institute of Physics) synchrotron in 1964 [14]. During the following four decades, a large number of theoretical and experimental works on the investigation and application of the ICE were accomplished (see [12, 15–18] and the literature therein). The advent of open resonators with a finess of 10^4–10^5 and repetitively pulsed lasers with a high mean power (up to 1kW) offered new opportunities of creating intense X-ray sources [15, 19–25]. In the next section, we analyze a possible construction of a medical X-ray diagnostic source based on the ICE.

3. PARAMETERS OF THE LASER-ELECTRON X-RAY SOURCE

An effective monochromatic X-ray source can be produced on the basis of a repetitively pulsed laser and an electron storage ring. The interaction between the laser and electron beams occurs in the rectilinear gap of the storage ring, which has a zero dispersion function [17]. The radiation damping and amplitude buildup of the betatron and phase oscillations associated with the Rayleigh resonance scattering by ions in this geometry were considered in [17, 18].

Let us determine at what parameters of the storage ring and laser one can obtain X-ray flux $\Phi \cong 10^{14}$ s^{-1}, which is required for solving medical problems (see Section 1).

The parameters of a relatively compact storage ring, which can be installed at a medical center or a specialized clinic, are listed in Table 1.

Using the data of Table 1 and determining the total number of electrons in the storage ring and in the beam cross section

$$N_e = ic/2\pi eR \cong 1.3 \times 10^{10},$$
$$S_0 = 2\pi\sigma_{x, z}^2 = 2.1 \times 10^{-5} \text{ cm}^2 \qquad (4)$$

we substitute these values into (3) and find the flux of X-ray photons

$$\Phi = 4.1 \times 10^{-10}\Phi_L \cong 4.1 \times 10^{-10}\frac{P_L}{\hbar\omega_L}, \qquad (5)$$
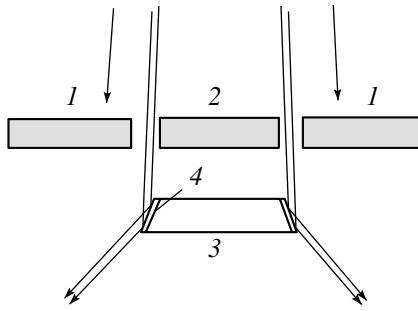
Fig. 2. Schematic diagram of spectral selection and diffraction sweep of the initial beam in the axial cross section: (*1*, *2*) annular aperture elements; (*3*) substrate with a conic surface; and (*4*) layer of oriented crystal monochromators.

Fig. 3. Schematic of a two-dimensional mechanical sweep of the X-ray beam over the specified area under study at two spectrum lines.

where P_L is the laser power. For the visible range, $\hbar\omega_L \approx 1$ eV, and we have

$$\Phi[\text{s}^{-1}] = 2.6 \times 10^9 P_L[\text{W}]. \qquad (6)$$

Thus, in the case of the storage ring considered, obtaining an X-ray beam necessary for the medical application requires a laser beam with a power $P_L \cong 10^5$ W.

The totality of the storage ring parameters listed in Table 1 assumes that cross-sectional size of the electron beam $\sigma_{x,z}$ are determined by the ICE, and electron–electron interaction can be neglected. It is correct in our case, if the peak power of the laser pulse is $P_L^c > 200$ GW. Under such conditions, the buildup and radiative damping of betatron and phase electron oscillations in the storage ring are determined mainly by the processes of scattering of laser-beam photons by electrons [15]. Let us assume that laser pulse length corresponds to the electron-bunch length $\tau_L = \sigma_\varphi/c \approx 1.4 \times 10^{-11}$ s. Since the laser pulse repetition rate coincides with the electron rotation frequency, the interval between laser pulses is $T_L = 2\pi R/c \approx 2 \times 10^{-8}$ s, where R is taken from Table 1. It is evident from here that, at the mean laser power $P_L = 10^5$ W, the peak power is $P_L \approx 1.4 \times 10^8$ W, i.e., this is three orders of magnitude lower than $P_L^c \approx 200$ GW.

The required laser peak power can be obtained in a high-quality-factor optical resonator. For this purpose, its length should be a half of the electron orbit perimeter and the finess $(1 - r)^{-1} \geq 2 \times 10^3$ is necessary, where r is the reflection coefficient of the mirrors. Obviously, introducing a resonator also proportionally increases the average power of X-ray radiation. As a result, the laser radiation should be represented by a sequence of pulse trains with a duration T_1 and an interval $T_2 = 2 \times 10^3 T_1$ between them. The parameters of an appropriate laser are listed in Table 2.

4. SYSTEM FOR OBTAINING PROJECTIONS USING LASER–ELECTRON SOURCES.

The suggested system for obtaining projections using laser–electron sources is shown in Fig. 1. The possibility of obtaining frontal and sagittal projections in the horizontal position of a patient is very important in medical practice. For ensuring the fulfillment of this condition, two electron storage rings H_1 and H_2 are positioned in the vertical plane. The axes of the optical resonators formed by the focusing mirrors M_1, M_2 and M_3, M_4 are vertically and horizontally oriented.

An electron synchrotron with an energy of 50 MeV, a linear accelerator, or a microtron, which is expedient to be placed in a basement, can be a source of electrons. Electrons can be injected into the storage rings singly or during several cycles through the injectors. The electron lifetime in the storage rings is 10–20 h. Therefore, injection cycles are repeated in several hours.

An X-ray beam is generated under the excitation of optical resonators with a finess of $\sim 2 \times 10^3$ by lasers L_1 and L_2 during the patient's examination. The instants of generation of optical pulses are synchronized with the rotation of the electron bunches in such a way that photons and electrons interact at the center of the resonator. Solid-state lasers based on YAG or Al_2O_3 : Ti, on which a mean power of >10 W is obtained in different regimes, can be used as optical generators [26].

The X-ray beam is quasi-monochromatic. X-ray beams are extracted from the resonator through membranes transparent for X rays and located at the center of the mirrors M_2 and M_4. Sweep systems P_1 and P_2 provide the transformation of the initial beam into a fan-shaped one (see Section 5). The radiation transmitted theough the patient is registered by the detecting units D_1 and D_2. A table T, on which a patient is placed, can move back and forth along the line perpendicular to the drawing plane.

5. X-RAY BEAM SWEEP

As follows from the formula for the angular distribution of the flux density [12], at an energy above 30 keV, the opening angle ψ of the generated X-ray beam (determined the half-height of the power distribution) is $\cong 20'$. This means that, at a distance of 10 m from the source, the size of the irradiated region is 5–6 cm. Therefore, to preserve the size of the diagnostic system acceptable from the practical viewpoint, it is necessary to provide the X-ray beam sweeping over the specified investigation zone. Two approaches are basically possible for solving this task: (1) a diffraction–mechanical sweep of the initial beam using a deflecting element and (2) deflection of the initial beam by altering the electron path with electromagnets located in the storage ring.

As an example, let us consider a variant of the diffraction–mechanical sweep. The axial section of the deflecting system and circular sweep of the initial beam using a layer of crystal monochromators is shown in Fig. 2. Since the photon energy distribution is axially symmetric, the diaphragm in a plane normal to the axis of the initial beam should be shaped as an annular slot, the width of which provides the selection of the specified spectral band. The substrate should have a shape of a truncated cone surface, on which the crystals are located. The reflecting surfaces of the crystals is tangent to the cone surface.

If the glancing angle between cone surface and the incident beam is θ_B, then the monochromator reproducing the shape of the substrate deflects the incident radiation by an angle $2\theta_B$. Such a monochromator can be produced of pyrolitic graphite, which, in compliance with the data [27] at $E = 30$ keV ($\lambda = 41$ pm), ensures a reflection coefficient of 0.25–0.35 for energies of 1–2 keV. At the distance H from the deflecting element in the plane normal to the axis of the initial beam, the irradiated region will be shaped as a ring with the radius $r_c = H\sin(2\theta_B + \psi/2)$.

Two coaxially located monochromators allow for the selection of two energy bands. The fact that they can be chosen on different sides from the K-jump in the absorption of a certain element principally allows one to obtain difference images of cavities and vessels, which are filled with a contrast substance, not shaded by other organs.

For obtaining usual images in the specified region, shown in Fig. 3 in the form of a smoothed rectangle, it is expedient to use a part of the ring zone selected by the diaphragm. The position of the radiation zones in the limiting positions, which are produced during linear scanning by two beams with the mean powers E_1 and E_2, is shown in Fig. 3. In the simplest case, the beam sweep over the investigated field is executed by mechanical scanning of the table with a patient relative to the radiation source. The radiation is detected by two detector units positioned along an arc, the design of which is similar to that of the detection systems of modern medical computerized tomographs. This allows one

to decrease a background of scattered radiation and thereby increase the image contrast and informativeness. Note that an instantaneous sweep of the initial annular beam over the total area of the zone of interest using a system of monochromators is possible in principle. However, this is an independent and rather complex task, which is not a topic of this work.

6. CONCLUSIONS

Let us enumerate the main advantages of the proposed scheme for obtaining images with a laser–electron radiation source in comparison with standard diagnostic systems based on X-ray tubes. They follow from the monochromaticity, high intensity, X-ray beam directivity, and from the possibility of sequentially scanning the beam over the investigated zone. The positive role of these factors in X-ray diagnostics has been experimentally confirmed using numerical computations by the Monte-Carlo simulation [6, 27, 28].

(1) A decrease in the total patient's radiation dose by monochromatizing the X-ray beam and selecting its optimal power (up to 30%).

(2) Elimination of the measurement errors concerned with the radiation polychromaticity during digital recording of X-ray projections. Without special algorithms for polychromaticity correction, the measurement errors of X-ray flux attenuation can reach $\sim 100\%$.

(3) Improvement of the useful signal-to-noise ratio (≥ 3) due to a reduction of the influence of rescattering effects in the object for the forward beam attenuated by a factor of $\geq 10^2$.

(4) The possibility of recording different object images on the K-jump of photoabsorption of the contrast substance in two energy-close spectral regions under continuous alteration of the field of vision.

(5) A decrease in the radiation background in workrooms with the equivalent power of the X-ray source preserved.

(6) The possibility of decreasing the mass of the radiation shielding by a factor of 2–3 without an increase in the absorbed dose for the personnel near the radiation source.

It should be also noted that, in comparison to experimental medical systems based on synchrotron sources, the system considered makes it possible to obtain both frontal and saggital projections at the horizontal position of a patient, thus lifting any restrictions related to the patient's state.

The aforementioned advantages are obviously significant in both the diagnostics for detection of pathologies at early stages of their formation and when conducting long and complex surgeries under the control of an X-ray visualization system.

REFERENCES

1. Blinov, N.N. and Mazurov, A.I., *Med. Tekh.*, 1999, no. 5, p. 3.
2. Chikirdin, E.G., *Med. Tekh.*, 1998, no. 3, p. 36.
3. Vasil'ev, V.N., Lebedev, L.A., Sidorin, V.P., and Stavitskii, R.V., *Spektry izlucheniya rentgenovskikh ustanovok. Spravochnik (*Radiation Spectra of X-ray Installations: Handbook), Moscow: Energoatomizdat, 1990.
4. Macovski, A., *Proc. IEEE*, 1983, vol. 71, no. 3, p. 373.
5. Herman, G.T., *Image Reconstruction from Projections: The Fundamentals of Computerized Tomography*, New York: Academic, 1980.
6. Mashkovich, V.P., *Zashchita ot ioniziruyushchikh izluchenii: Spravochnik* (Protection against Ionizing Radiation: A Handbook), Moscow: Energoatomizdat, 1982.
7. Dyson, N.A., *X-Rays in Atomic and Nuclear Physics*, London: Longman, 1973.
8. Blokhin, M.A., *Fizika rentgenovskikh luchei* (X-ray Physics), Moscow: GITTL, 1957.
9. Blokhin, M.A. and Shveitser, I.G., *Rentgenospektral'nyi spravochnik* (Handbook on X-ray Spectra), Moscow: Nauka, 1982.
10. *PersT*, 2001, vol. 8, no. 8, p. 6.
11. *CERN Courier News, Medicine*, 2001, p. 8.
12. Bessonov, E.G., *Tr. Fiz. Inst. im. P.N. Lebedeva, Ross. Akad. Nauk*, 1993, vol. 214, p. 3.
13. Landeker, K., *Phys. Rev.*, 1952, vol. 86, no. 6, p. 852.
14. Kulikov, O.F., Tel'nov, Yu.A., Filippov, E.I., and Yakimenko, M.N., *Zh. Eksp. Teor. Fiz.*, 1964, vol. 47, p. 1591.
15. Zhirong Huang and Ruth, R.D., *Phys. Rev. Lett.*, 1998, vol. 80, no. 5, p. 976.
16. Bessonov, E.G., *J. Russ. Laser Res.*, 1994, vol. 15, no. 5, p. 403.
17. Bessonov, E.G. and Kwang-Je Kim, *Phys. Rev. Lett.*, 1996, vol. 76, no. 3, p. 431.
18. Bessonov, E.G. and Kwang-Je Kim, Abstracts of Papers, *V European Particle Accelerator Conf.*, Barcelona: Sitges, 1996, vol. 2, p. 1196.
19. Chen, J., Imasaki, K., Fujita, M., *et al.*, *Nucl. Instrum. Methods Phys. Res. A*, 1994, vol. 341, p. 346.
20. Nakajima, K., Abstracts of Papers, *Advance Accelerator Concepts: VIII WS*, Lawson, W., Bellamy, C., and Brosius, D., Eds., Baltimore, Maryland, 1998, p. 280.
21. Gladkikh, P., Karnaukhov, I., Kononenko, S., and Shcherbakov, A., *Nucl. Instrum. Methods Phys. Res. A*, 2000, vol. 448, p. 41.
22. Agafonov, A.V., Botman, J., Gladkikh, P.I., *et al.*, *Probl. At. Sci. Technol. Ser. Nucl. Phys. Invest.*, 2001, no. 1, p. 126.
23. Urakawa, J., Uesaka, M., Hasegawa, M., *et al.*, Abstracts of Papers, *ICFA-2001 Beam Dynamic WS*, New York: Stoni Brook, 2001 (in press).
24. Bessonov, E.G., Abstracts of Papers, *ICFA 2001 Beam Dynamic WS*, New York: Stoni Brook, 2001 (in press).
25. Litvinenko, V.N., Shevchenko, O.A., Mikhailov, S.F., *et al.*, Abstracts of Papers, *2001 Particle Accelerator Conf.*, Chicago: IL, 2001.
26. Kryukov, P.G., *Kvantovaya Elektron.* (Moscow), 2001, vol. 31, no. 2, p. 95.
27. Freund, A.K., Munkholm, A., and Brennan, S., *Proc. SPIE*, 1996, vol. 2856, p. 68.
28. Gurvich, A.M., *Fizicheskie osnovy radiatsionnogo kontrolya i diagnostiki* (Physical Fundamentals of Radiation Control and Diagnostics), Moscow: Energoatomizdat, 1989.